Available online at www.sciencedirect.com
ScienceDirect
Optics and Lasers in Engineering 47 (2009) 403–411
OPTICS and LASERS in ENGINEERING
www.elsevier.com/locate/optlaseng

On the feasibility of optical fibre sensors for strain monitoring in thermoplastic composites under fatigue loading conditions

I. De Baere*, G. Luyckx, E. Voet, W. Van Paepegem, J. Degrieck

Department of Mechanical Construction and Production, Faculty of Engineering, Ghent University, Sint-Pietersnieuwstraat 41, B-9000 Gent, Belgium

Available online 12 February 2008

Abstract

This study investigates the possibility of using optical fibres with Bragg gratings for measurements in thermoplastic composites under fatigue loading conditions. Two setups are considered: (i) the fibre is embedded in the composite and (ii) the grating is bonded externally. Detailed information is given on the principle of optical fibre measurements and the data acquisition for both setups. To verify the strain derived from the optical fibre, the strain is compared with extensometer measurements. A special design of the blades of the extensometer is presented, since the standard blades suffer from a loss of grip on the surface of the specimen. The material used for this study was a carbon fibre-reinforced polyphenylene sulphide.

It can be concluded for both setups that the optical fibre survives over half a million loading cycles, without de-bonding of the fibre. The advantage of the external fibre over the embedded one is that it can be mounted after manufacturing of the plate, but it has a higher risk of being damaged during working conditions of the component.

Keywords: Fibre Bragg grating; Thermoplastic composites; Fatigue

1. Introduction

When performing experiments, both under quasi-static or fatigue loading conditions, in order to determine the mechanical properties of material, such as Young's modulus, Poisson's ratio, fatigue lifetime, … the strain is usually measured with extensometers or strain gauges. For this study, optical fibre Bragg gratings (FBG's) with special Organic Modified Ceramic (ORMOCER) coating and high mechanical strength are assessed for their ability to measure strain under fatigue loading conditions.

An average optical fibre is about 125 μm in diameter, which is about 10 times as much as the average carbon fibre (10 μm). Because of the load carrying capability however, they have limited influence on the mechanical behaviour if they are embedded.

The feasibility of optical fibre sensors for monitoring the mechanical behaviour is already studied in Refs. [1,2] for a thermosetting matrix, with good result. It was even concluded that optical fibre Bragg sensors were more reliable than classical strain gauges [1]. Doyle et al. [3] experimented on the use of fibre optic sensors for tracking the cure reaction of a fibre-reinforced epoxy, with success. They also successfully demonstrated the feasibility of these sensors for monitoring the stiffness reduction due to fatigue damage, but for thermosetting matrix. The latter was also done by C.S. Shin and C.C. Chiang for a carbon fibre-reinforced epoxy [4,5].

The authors had already done some preliminary tests on the use of optical fibres for fatigue measurements [6]. In that manuscript, an swept laser interrogator (SLI) was used for the optical data acquisition, which proved not to be very convenient, since the fatigue test had to be stopped manually to perform quasi-static tests.

In this study, a newly developed data acquisition system is presented, which combines the optical data acquisition with the control of the tensile testing machine. This allows the user to specify the fatigue and quasi-static testing parameters and then the test can be performed without the necessity of further manual intervention. Furthermore, the option of an externally bonded grating is investigated, since

*Corresponding author. Tel.: +32 9 264 32 55; fax: +32 9 264 35 87.
E-mail address: Ives.DeBaere@UGent.be (I. De Baere).

0143-8166/$ - see front matter © 2008 Elsevier Ltd. All rights reserved.
doi:10.1016/j.optlaseng.2008.01.001

this had the advantage of being attached after fabrication of a composite part. Normally, fibres are embedded in the composite part at locations where measurements are deemed necessary. If it is decided afterwards that extra sensors are needed at specific locations, they can no longer be embedded in the already cured part.

For this manuscript, a carbon fabric-reinforced thermoplastic, namely a polyphenylene sulphide (PPS), is investigated. Since PPS is known for its chemical inertness, debonding of the fibre, both embedded and external, may be a problem.

In the following paragraph, the principle of fibre Bragg gratings is discussed. Then, some details are given about the material under study and the optical data acquisitions. This is followed by the fatigue experiments and finally, some conclusions are drawn.

2. Fibre Bragg grating sensors

The principle of an optical fibre sensor with a Bragg grating is illustrated in Fig. 1. Broadband light is transmitted into the optical fibre. At a specific point in this fibre, there is a Bragg grating, which acts as a wavelength selective mirror. For each grating only one wavelength, the Bragg wavelength, λ_B is reflected with a full width at half maximum of typically 100 pm, while all other wavelengths are transmitted. As a result, an optical fibre can be read out from both ends of the fibre. A detailed image of such grating is given in Fig. 1 (right).

A FBG is actually no more than an area in the core of the fibre with successive zones with an alternating refractive index. If Λ is the period of the grating, then the Bragg wavelength of the grating is given by:

$$\lambda_B = 2n_{eff}\Lambda, \tag{1}$$

where n_{eff} is an averaged refractive index over the length L of the grating. If strain is imposed on the grating, the length Λ changes. As such, a measurement of the strain is achieved: the difference between the wavelength of the strained and the unstrained grating increases linearly with the imposed strain (Eq. (2)):

$$\left.\begin{matrix}\varepsilon_1 \sim \Lambda_1 \sim \lambda_1 \\ \varepsilon_2 \sim \Lambda_2 \sim \lambda_2\end{matrix}\right\} \rightarrow \Delta\varepsilon \sim \Delta\lambda. \tag{2}$$

The isothermal strain sensitivity is given by

$$\frac{\Delta\lambda_B}{\lambda} = \left[1 - \left(\frac{n_{eff}^2}{2}\right)(p_{12} - v(p_{11} + p_{12}))\right]\varepsilon_{zz}, \tag{3}$$

where ε_{zz} is the strain induced in axial direction of the optical fibre, n is the refractive index, v is the Poisson's ratio and p_{11} and p_{12} are the elasto-optic coefficients of the elasto-optic tensor. Some material constants used to calculate the strain sensitivity of GeO_2 doped silica glass-fibre are (Table 1):

Introducing these material constants in Eq. (3) yields:

$$\frac{\Delta\lambda_B}{\lambda} = 0.796\varepsilon_{zz}. \tag{4}$$

A strain sensitivity coefficient of 1.2 pm per microstrain is found at the operating wavelength of 1.5 μm.

This is an absolute value, since it only depends on the geometry of the grating and the elasto-optic constants of the glass, and not on any form of electronic manipulation such as filtering or amplifying. As such, it does not drift away in time, as can be the case with strains, derived from strain gauge measurements.

It should be noted that the temperature sensitivity is not discussed in this paper, because previous experiments [6] have shown that during fatigue experiments on the material under study, no heat is generated. The temperature sensitivity is discussed by the authors in Ref. [6].

The choice of the characteristic wavelength λ_B depends on the type of experiment and the data acquisition unit. The latter will be able to register only a certain range of wavelengths and has a certain bandwidth in the C-band region (1527–1567 nm) that is determined by the optical source of the interrogator. If the experiment is pure tension, λ_B should be chosen near the lower boundary of that range and if the experiment is pure compression, λ_B should be chosen near the upper boundary of that range. The outer boundary should not be chosen, since the

Table 1
Material constants of the glass fibre

n_{eff}	v	p_{11}	p_{12}
1.45	0.16	0.113	0.252

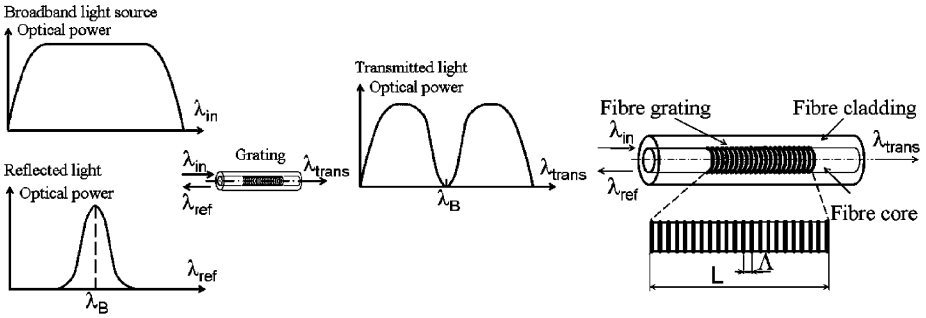

Fig. 1. The principle of an optical fibre Bragg grating (FBG) (left) and detail of the grating (right).

production process, in this case hot pressing, introduces unknown stresses and as a result, a small shift in λ_B [1,7].

The fibre optic sensors used for these embedding experiments are Draw Tower fibre Bragg gratings. Such gratings are manufactured during the fabrication process of the optical fibre and are coated just after the inscription of the Bragg grating [8]. The FBG's are written in a single mode optical fibre with core diameter of 6 μm and cladding diameter of 125 μm and they have a typical length of about 8 mm. Such a single mode fibre is made of fused silica (SiO_2) with a Ge-doped core for high photosensitivity, necessary for inducing the periodic refractive index pattern and thus creating the Bragg grating. The size of FBG's is comparable with that of a carbon fibre bundle (approximately 320 μm) and they are coated with an ORMOCER coating of 195 μm.

This coating material provides excellent mechanical properties such as an ultimate strain value between 5% and 6%. It should be noted that the ORMOCER has good bonding properties with the glass surface of the optical fibre and therefore this optical fibre has very good sensor properties for strain measurements. Also a good adhesion with the PPS matrix is found, even after half a million cycles the FBG-sensors showed no signs of de-bonding (see Section 3.3).

3. Materials and methods

3.1. Composite material

The material used for the experiments was a 5-harness satin-weave carbon fabric-reinforced PPS. The carbon PPS plates were hot pressed, one stacking sequence was used for this study, namely $[(0^\circ, 90^\circ)]_{2s}$ where $(0^\circ, 90^\circ)$ represents one layer of fabric.

The in-plane elastic properties of the individual carbon PPS lamina were determined by the dynamic modulus identification method as described in Ref. [9], the tensile strength properties were determined at the Technical University of Delft. A summary is given in Table 2.

The test coupons were cut with a water-cooled diamond saw. The dimensions of the coupons used for fatigue experiments were chosen according the ASTM D3479 standard for tension–tension fatigue and are shown in Fig. 2 for the specimen with the embedded fibre. It was attempted to have the grating of the fibre somewhere in the middle. The same dimensions where used for the other setup with the external optical fibre. Fig. 3 shows an example of such a specimen.

Table 2
In-plane elastic properties of the individual carbon/PPS lamina (dynamic modulus identification method)

E_{11} (GPa)	56.0
E_{22} (GPa)	57.0
ν_{12} (dimensionless)	0.033
G_{12} (GPa)	4.175
X_T (MPa)	736
ε_{11}^{ult} (dimensionless)	0.011
Y_T (MPa)	754
ε_{22}^{ult} (dimensionless)	0.013
S_T (MPa)	110.0

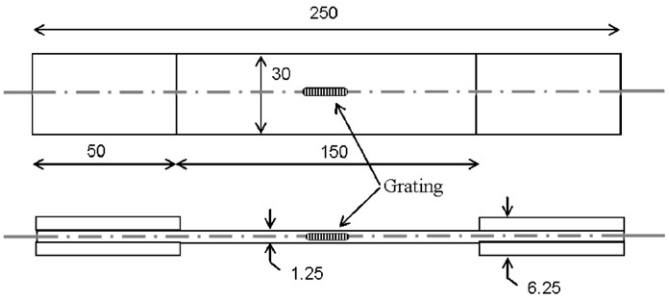

Fig. 2. Dimensions of the used tensile coupon, equipped with tabs.

Fig. 3. Tensile coupon with embedded optical fibre, equipped with glass-PEI tabs.

3.2. Tensile testing machine

All tensile tests were performed on a servo-hydraulic INSTRON 8801 tensile testing machine with a FastTrack 8800 digital controller and a load cell of ± 100 kN.

For the strain measurements, strain gauges could not be used, since they tend to de-bond after a few thousands of cycles. Furthermore, PPS is not easily glued. Therefore, an extensometer was mounted on the specimen. The blades of the extensometer however, tended to loose grip on the very smooth surface of the thermoplastic composite. A different design of the blades was used, which is illustrated in Fig. 4 (right). The pointed blades always make a good contact with the specimen, since three points define a surface. Furthermore, the width of the blades is in better correspondence with the width of the used tensile specimens.

For the registration of the tensile data, a combination of a National Instruments DAQpad 6052E for FireWire, IEEE 1394 and the SCB-68 pin shielded connector were used. The load, displacement and strain, given by the FastTrack controller were sampled on the same time basis.

3.3. Optical data acquisition

In Ref. [6], the authors have used an SLI for the optical data acquisition. This was not convenient since the fatigue test had to be stopped manually to perform quasi-static tests.

For this study, the optical data acquisition is combined with the control of the tensile testing machine. Using the 'Wavemaker' and 'Waverunner' software from Instron™, the user is able to specify any waveform, or successive

waveforms. The waveform used here is composed out of a static test and a fatigue test, both load-controlled. For the fatigue test, the only parameters are the average load, the amplitude and the frequency. The static test is implemented as a multistage evolution of the load, which is illustrated in Fig. 5. The user has to implement the step-height, step-time and the number of steps (500 N, 150 s and 10 steps in the presented figure).

The optical data are registered by the FBG-scan interrogator, which is monitored by a computer. This computer also monitors the strain, load and displacement given by the tensile machine. If the load remains constant for a certain period of time, which is the case in the multistage static test, but not in the fatigue test, all of the data, both from the FBG-scan as from the tensile machine, are written to file. As such, all static tests are automated and registered without the necessity of further human intervention and all data are written on the same time basis.

The FBG-scan interrogator is a portable device that can monitor up to 16 different optical lines. The core of the device is a state-of-the-art Fabry Pérot tuneable filter. It features a wavelength accuracy of 10 pm and a scan range of 40 nm, from 1527 nm till 1567 nm. The wavelength repeatability is 1 pm, and the scan and report time is 1 s, representing a sampling rate of 1 Hz in total. The latter means that it takes 1 s to scan one channel, so if two gratings are read, the sampling frequency of each channel is 0.5 Hz.

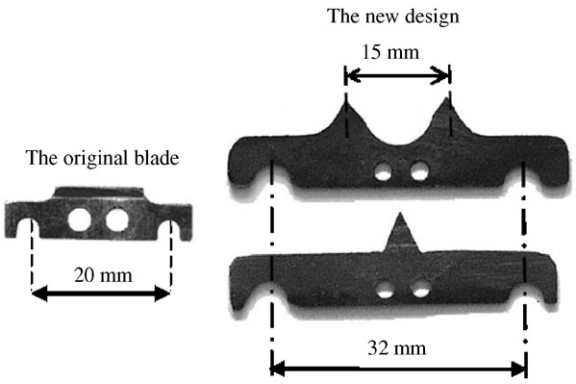

Fig. 4. Illustration of the extensometer blades.

4. Experiments and discussion

4.1. The embedding of the fibre

If we consider composite material with embedded optical fibres, it is important that there is minimal or no disturbance of the composite's structural behaviour. Thin plates compiled of four laminae were used to investigate if the optical fibre showed any significant influence on the material properties.

These plates with $[(0^\circ, 90^\circ)]_{2s}$ stacking sequence are fabricated by stacking a number of semi-preg layers (with reinforcement fibres woven in 0° and 90°) and by pressing it together with appropriate pressure and temperature. Optical fibres can be put in between two layers of semi-preg and can the grating can be fixated in any orientation simply by using an ultrasonic welding device and a small piece of PPS-sheet to fix the fibre at the semi-preg layer.

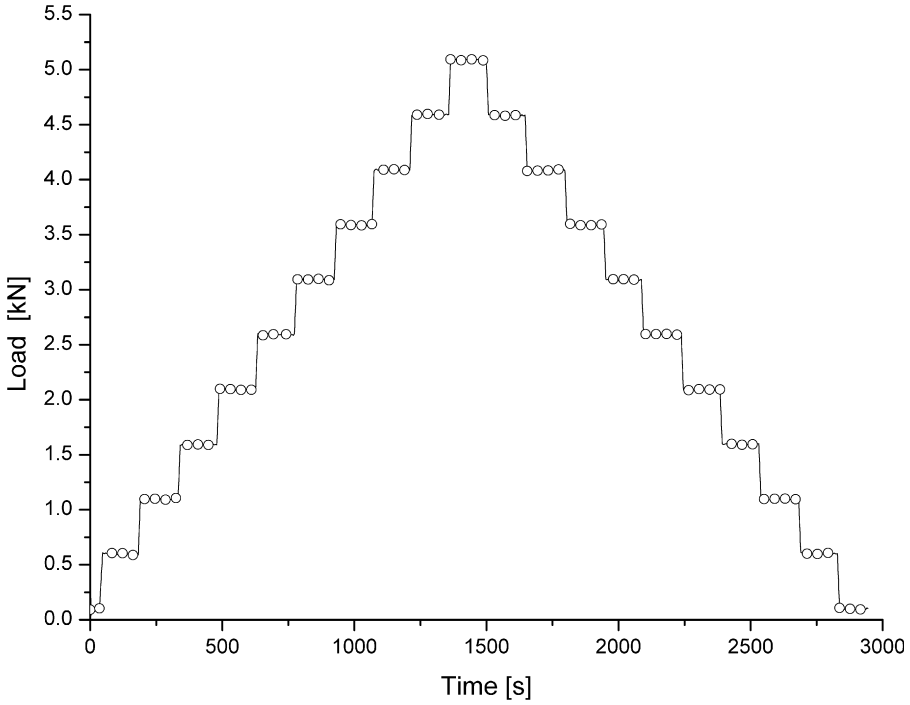

Fig. 5. Illustration of the evolution of the force during the optical data acquisition.

Of course, the fragile optical fibre needs to be protected where it exits the specimen. This was achieved by using Kapton tape on the sides of the semi-pregs where the fibre exited the specimen. The fibres were also fixated by taping them with an extra piece of Kapton tape on the underlying layer of tape. Both systems are illustrated in Fig. 6; Fig. 7 shows the protection of the Kapton tape on the exiting fibre after the plate is cured.

This curing was done by pressing the layers together in a hot mould at a pressure of 10 bar and temperature of approximately 320 °C for a few hours and further cooling off with air- and water-cooling till room temperature.

Considering the dimensions of such semi-preg layers (thickness approximately 320 μm), one would say optical fibres with a coating diameter of 195 μm could induce local disturbance in the matrix and influence the structural behaviour of the composite. However, fatigue tension tests showed positive results indicating that the fibre optic sensor has little or nil effect on the mechanical properties of the composite plate [6].

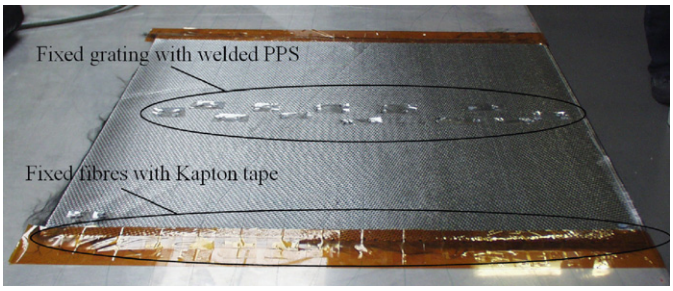

Fig. 6. Illustration of how both gratings and fibres can be fixated.

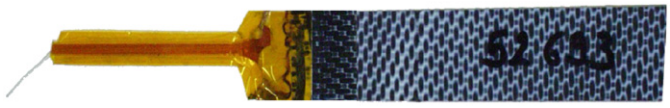

Fig. 7. A fibre, protected by the Kapton tape, exiting the specimen.

In addition, the coating of the optical fibre should have a good adhesion with the matrix-material, so that strain inside the composite is transmitted well. The ORMOCER coating showed a good transmission of strain to the draw tower grating (DTG®) and there was no significant difference in mechanical properties in comparison with samples without embedded optical fibre [6].

Finally, Fig. 8 shows the change in spectrum resulting from the embedding process. As can be noted, there is a shift to the right from 1548.577 to 1549.47 nm, yielding a strain of 744 microstrain. Furthermore, losses in power have occurred due to macro-bending on entrance of the plate and micro-bending inside the plate.

Changes in reflected spectra after consolidation are known to happen in epoxy-matrices [10–12], but has also been documented for the thermoplastic matrix PPS in Ref. [13].

4.2. Bonding the external fibre to the surface

If the external fibre is bonded on the surface, then no disturbance of the composite will occur. The followed procedure is the same as for bonding strain gauges. First, the surface of the specimen was polished in order to have a smooth surface, after which it was degreased with acetone. Then, the fibre was accurately positioned and pre-strained, before being fixed to the specimen by means of duck tape. The pre-strain caused a shift of about 100–200 pm corresponding with a strain of 80–160 microstrain. This was done to avoid buckling of the fibre when the specimen is unloaded.

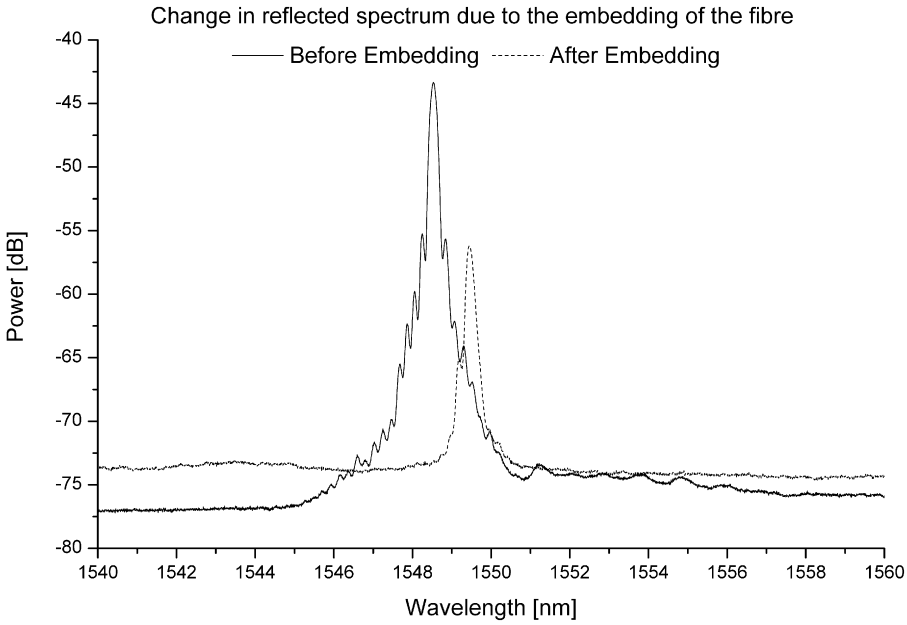

Fig. 8. Illustration of the reflected spectrum prior and after the embedding process.

Finally, the fibre was bonded over the entire length of the grating, using a Z70 cyanide-acrylate adhesive, designed for bonding strain gauges. Extra pressure for the curing of the adhesive was applied, using a piece of soft rubber that morphs around the fibre and a Teflon film to avoid the rubber from bonding to the specimen and the fibre.

An image of an externally bonded fibre is given in Fig. 9.

4.3. Fatigue experiment

4.3.1. Embedded fibre

To assess whether the optical fibre is capable of measuring strains during the entire lifetime of the composite specimen, several fatigue tests were performed.

The first test presented here is done on a specimen with only an embedded optical fibre. It is a force controlled test with σ_{max} equal to 300 MPa, which is about 50% of the

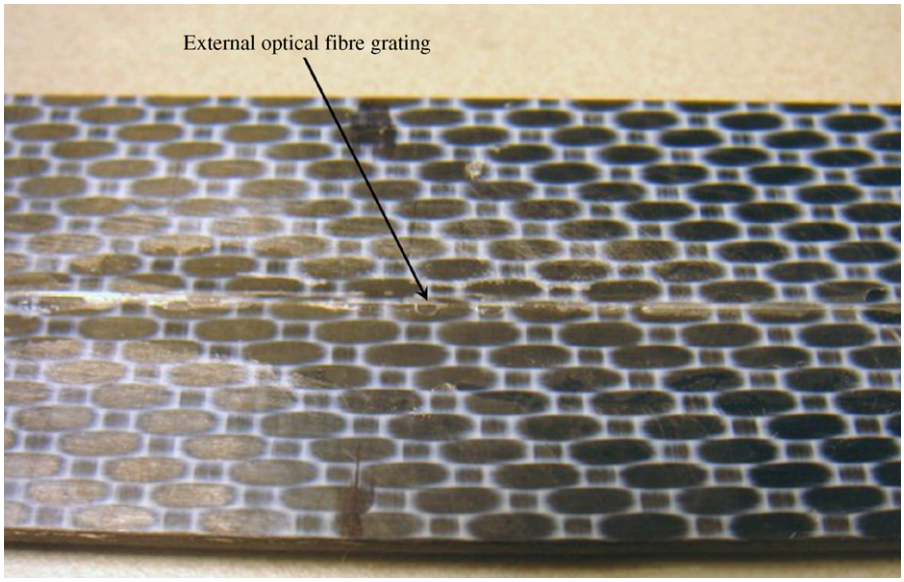

Fig. 9. Detailed image of an externally bonded optical fibre.

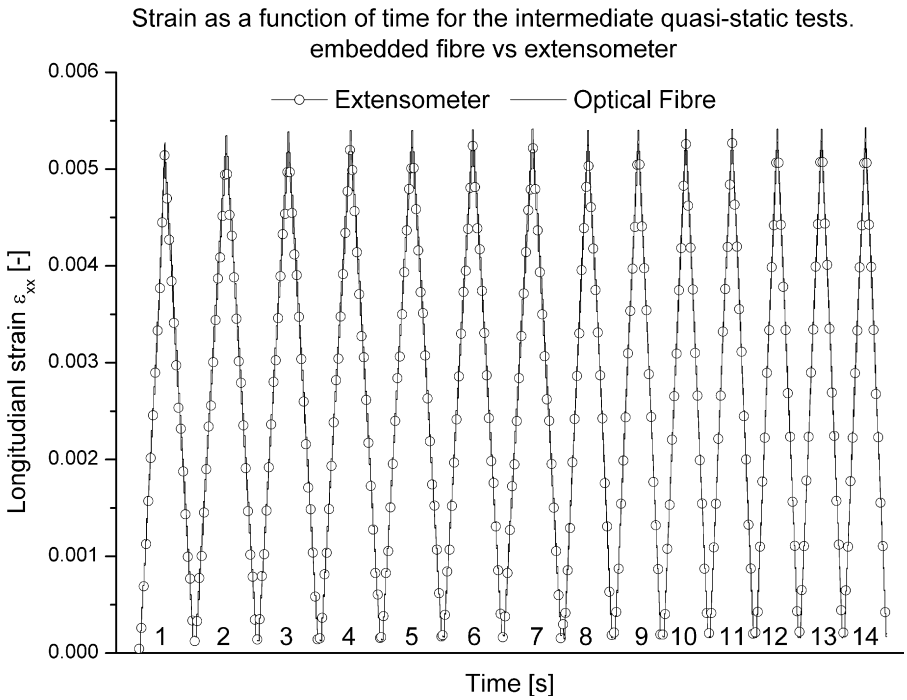

Fig. 10. Comparison of the different longitudinal strains, as a function of the time for the successive quasi-static tests for the specimen with the embedded optical fibre.

ultimate tensile stress, σ_{min} equal to 0 MPa and with a loading frequency of 5 Hz. The latter is a compromise between (i) heat generation, which occurs at higher frequencies and (ii) duration of the test. This experiment was paused every 40,200 cycles to perform a load controlled static test, as described in Section 3.3. In total, 14 static tests were done and then the specimen was removed from the tensile machine, so it could be examined further; the specimen had not failed. The embedded optical fibre had a starting wavelength of 1549.5 nm.

Fig. 10 illustrates the measured strains of these static tests, both with the extensometer and the optical fibre. The strain from both loading and unloading is plotted as a function of the time (s), the 14 different curves are given a certain small offset with respect to each other, to have a clear image. Underneath each measurement, the corresponding cycle is noted; the first curve corresponds with the initial static test. It may be remarked that the results correspond perfectly.

The stress–strain curves, corresponding with these static tests, are shown in Fig. 11, together with the corresponding stiffness. It must be noted that there is almost no stiffness degradation and only very limited permanent deformation, even after more than half a million cycles. This permanent deformation was also measured by the optical fibre, as can be seen in Fig. 10. In Ref. [5], a significant stiffness reduction was found, but for a carbon fibre-reinforced epoxy. It may be noticed that the stiffness increases after the seventh tensile test, but this is due to scatter on the measurement and it is visible because of the very small stiffness degradation.

Since it is difficult to distinguish the different curves and the amount of permanent deformation, these values are given in Table 3. It should be noted that these values correspond well.

4.3.2. External fibre

To assess whether an optical fibre grating could also be used as an external sensor, an extra specimen was prepared with an external optical fibre. The external optical fibre had a starting wavelength of 1540,531 nm. This fatigue test was also done with a maximum tensile stress of 300 MPa with a loading frequency of 5 Hz and the minimum stress was also 0 MPa. Six quasi-static tests were done to verify if the external fibre measured accurately. The first was done before the start of the fatigue test, the four intermediate tests were done, each after 100,000 and after 500,000 cycles,

Table 3
Permanent deformation after each unloading for the specimen with the embedded fibre

Cycle no.	Extensometer	Optical fibre
0	0.000124	0.000124253
40,200	0.000122	0.00016092
80,400	0.000136	0.000119253
120,600	0.000157	0.000126753
160,800	0.00017	0.000134253
201,000	0.000185	0.000165086
241,200	0.000151	0.000180086
281,400	0.000181	0.000157586
321,600	0.000202	0.000170086
361,800	0.000191	0.000164253
402,000	0.000201	0.000162586
442,200	0.000209	0.000160086
482,400	0.000219	0.000157586
522,600	0.000202	0.000170086

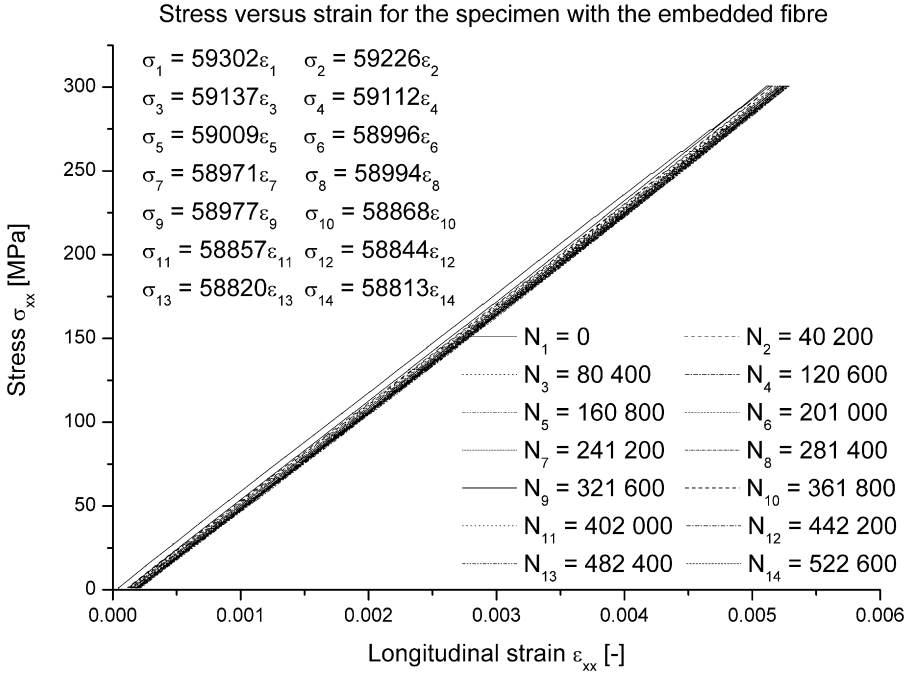

Fig. 11. Longitudinal stress as a function of the longitudinal strain for the different static tests for the specimen with the embedded optical fibre.

the specimen was loaded until failure. The corresponding strain curves from extensometer and external grating are plotted in Fig. 12. Both loading and unloading cycles are depicted; the different static tests are given a small offset for a clear image. It may be remarked that again there is perfect correspondence between the optical fibre and the extensometer.

The corresponding stress–strain curves are plotted in Fig. 13. Again, only limited permanent deformation and stiffness degradation occurs. It may be noted that the stiffness is less than for the specimen with the embedded FBG, but this is due to scatter on the results. In the last static test, after 500,000 cycles, a load of 327 MPa was reached before the specimen failed in the

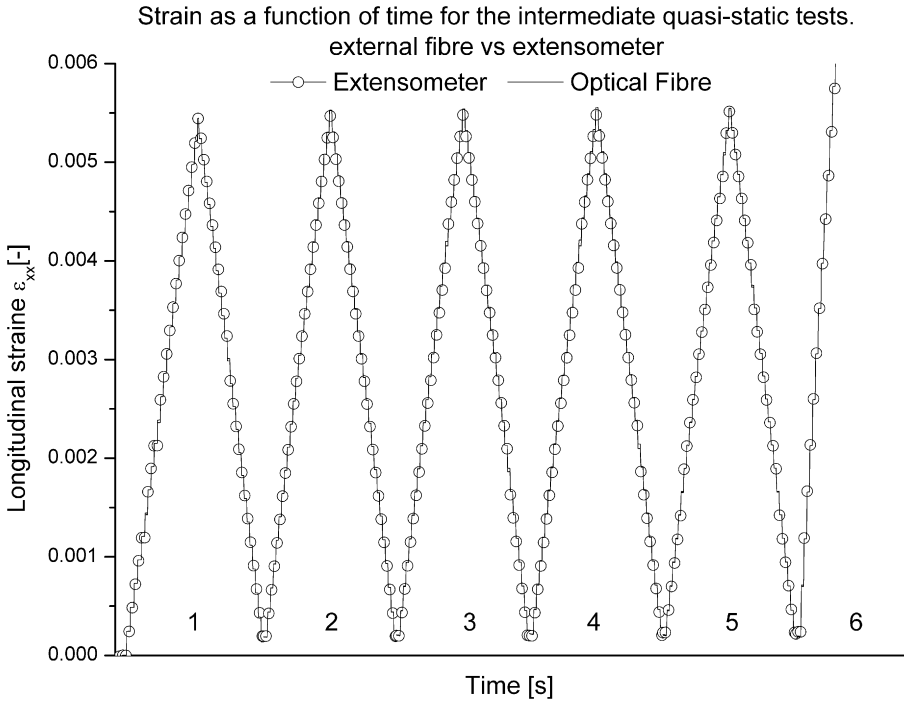

Fig. 12. Comparison of the different longitudinal strains, as a function of the time for the successive quasi-static tests for the specimen with the external grating.

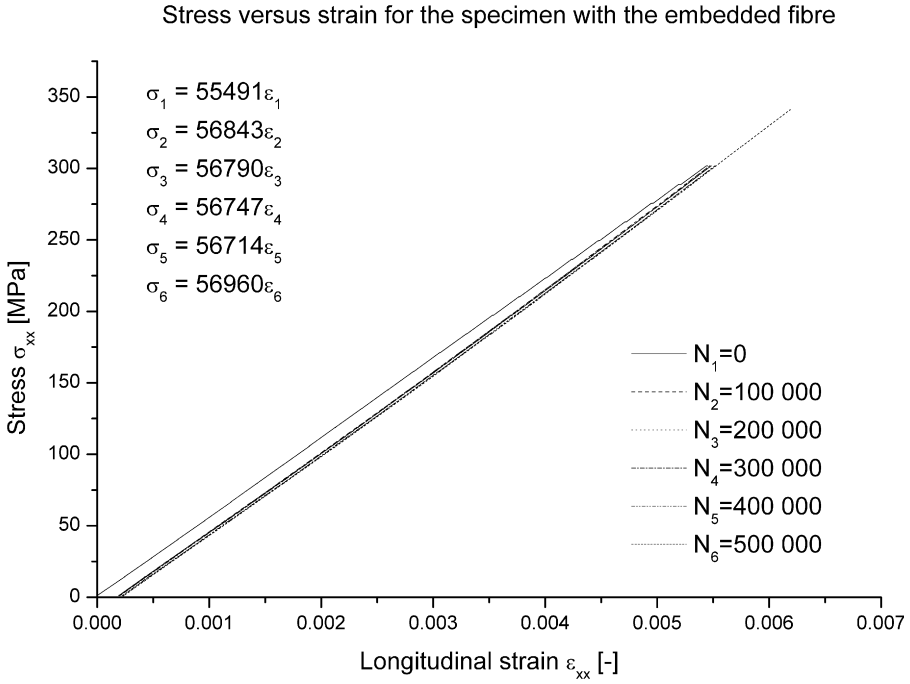

Fig. 13. Longitudinal stress as a function of the longitudinal strain for the different static tests for the specimen with the external optical fibre.

Table 4
Permanent deformation after each unloading for the specimen with the external fibre

Number of cycles	Extensometer	Optical fibre
0	0.000274	0.000137576
100,000	0.000298	0.000157576
200,000	0.000295	0.000186742
300,000	0.000303	0.000200909
400,000	0.000305	0.000210076
500,000	0.000333	0.000201742

tabs, which means this value is an underestimation of the residual strength.

Again, it is rather difficult to distinguish the different curves, so the residual strain after unloading is given in Table 4. Here, the correspondence is less than for the embedded fibre (Table 3).

In conclusion, future research on higher tension levels is necessary to examine whether the optical fibre does not de-bond and gives accurate measurements under these conditions, but the first results are very promising.

5. Conclusions

It may be concluded that embedded optical fibres in thermoplastic composites survive over half a million fatigue cycles, which is a lot more than strain gauges which tend to de-bond. The combined setup of INSTRON and FBG-scan interrogator automate the process, but if high sampling rates are required to measure the wavelength during dynamic loading, another setup/device will be necessary which operates at the sample and hold principle.

Since the surface of the used composite is very smooth, a special design of the extensometer blades was presented. These blades have a better grip on the surface of the specimen and therefore, no shifts in the strain measurement occurred during the fatigue loading. The latter was the case with the original blades, making strain-controlled tests unreliable.

The external fibre has the advantage of being mounted on any specimen after the production, there where the embedded one must be placed before manufacturing. On the other hand, the embedded fibre is less likely to be damaged. Both setups give promising results for fatigue tests with low maximum stress level. However, future research on higher tension levels is necessary.

Acknowledgements

The authors are highly indebted to the University Research Fund BOF (Bijzonder Onderzoeksfonds UGent) for sponsoring this research, to TenCate Advanced Composites for supplying the material, to FOS&S for their material and expertise and to FBGS-Technologies GmbH, Jena, Germany, for supplying the draw tower gratings.

References

[1] De Waele V, Degrieck J, Moerman W, Taerwe L, De Baets P. Feasibility of integrated optical fibre sensors for condition monitoring of composite structures—Part I: Comparison of Bragg-sensors and strain gauges. Insight 2003;45(April (4)):266–71.

[2] Degrieck J, De Waele W, Verleysen P. Monitoring of fibre reinforced composites with embedded optical fibre Bragg sensors, with application to filament wound pressure vessels. NDT E Int 2001; 34(June (4)):289–96.

[3] Doyle C, Martin A, Liu T, Wu M, Hayes S, Crosby PA, et al. In-situ process and condition monitoring of advanced fibre-reinforced composite materials using optical fibre sensors. Smart Mater Struct 1998;7(April (2)):145–58.

[4] Shin CS, Chiang CC. Embedded fibre Bragg grating sensors for internal fatigue damage monitoring in polymeric composites, advanced nondestructuve evaluation I, PTS 1 and 2. Proc Key Eng Mater 2006;321–323:230–3.

[5] Shin CS, Chiang CC. Fatigue damage monitoring in polymeric composites using multiple fiber Bragg gratings. Int J Fatigue 2006; 28(October (10)):1315–21.

[6] De Baere I, Voet E, Van Paepegem W, Vlekken J, Cnudde V, Masschaele B, et al. Strain monitoring in thermoplastic composites with optical fibre sensors: embedding process, visualization with micro-tomography and fatigue results. J Thermoplast Compos 2007; 20:453–72.

[7] Grattan KTV, Meggitt BT. Optical fibre sensor technology: fundamentals. Boston/Dordrecht/London: Kluwer Academic Publishers; 2000.

[8] Chojetzki C, Rothhardt M, Müller H-R, Bartelt H. Large fibre Bragg grating arrays for monitoring applications—made by drawing tower inscription, IPHT, Jena, Germany and FOS&S, Geel, Belgium; 2005.

[9] De Baere I, Van Paepegem W, Degrieck J, Sol H, Van Hemelrijck D, Petreli A. Comparison of different identification techniques for measurement of quasi-zero Poisson's ratio of fabric reinforced laminates. Composites, Part A 2007;38(9):2047–54.

[10] Colpo F, Humbert L, Botsis J. Characterisation of residual stresses in a single fibre composite with FBG sensor. Compos Sci Technol 2007;67(July (9)):1830–41.

[11] Montanini R, D'Acquisto L. Simultaneous measurement of temperature and strain in glass fiber/epoxy composites by embedded fiber optic sensors: I. Cure monitoring. Smart Mater Struct 2007; 16(October (5)):1718–26.

[12] Colpo F, Humbert L, Glaccari P, Botsis J. Characterization of residual strains in an epoxy block using an embedded FBG sensor and the OLCR technique. Compos A—Appl Sci Manuf 2006;37(4): 652–61.

[13] Sorensen L, Gmur T, Botsis J. Residual strain development in an AS4/PPS thermoplastic composite measured using fibre Bragg grating sensors. Compos A—Appl Sci Manuf 2006;37(2): 270–81.